Anomalous Dynamics of QBO Disruptions Explained by 1D Theory with External Triggering

AARON MATCH[a] AND STEPHAN FUEGLISTALER[a,b]

[a] *Program in Atmospheric and Oceanic Sciences, Princeton University, Princeton, New Jersey*
[b] *Department of Geosciences, Princeton University, Princeton, New Jersey*

(Manuscript received 8 June 2020, in final form 2 November 2020)

ABSTRACT: The quasi-biennial oscillation (QBO) is an alternating, descending pattern of zonal winds in the tropical stratosphere with a period averaging 28 months. The QBO was disrupted in 2016, and arguably again in 2020, by the formation of an anomalous easterly shear zone, and unprecedented stagnation and ascent of shear zones aloft. Several mechanisms have been implicated in causing the 2016 disruption, most notably triggering by horizontal eddy momentum flux divergence, but also anomalous upwelling and wave stress. In this paper, the 1D theory of the QBO is used to show how seemingly disparate features of disruptions follow directly from the dynamics of the QBO response to triggering. The perturbed QBO is interpreted using a heuristic version of the 1D model, which establishes that 1) stagnation of shear zones aloft resulted from wave dissipation in the shear zone formed by the triggering, and 2) ascent of shear zones aloft resulted from climatological upwelling advecting the stagnant shear zones. Obstacles remain in the theory of triggering. In the 1D theory, the phasing of the triggering is key to determining the response, but the dependence on magnitude is less steep. Yet in MERRA-2, there are triggering events only 20% weaker than the 2016 triggering and equal to the 2020 triggering that did not lead to disruptions. Complicating matters further, MERRA-2 has record-large analysis tendencies during the 2016 disruption, reducing confidence in the resolved momentum budget.

KEYWORDS: Quasibiennial oscillation; Stratospheric circulation; Vertical motion; Stratosphere-troposphere coupling; Climate variability; Reanalysis data

1. Introduction

The quasi-biennial oscillation (QBO) is an alternating, descending pattern of zonal winds in the tropical stratosphere with a period averaging 28 months (e.g., Baldwin et al. 2001). The QBO is driven by interactions between vertically propagating waves and the mean flow, which produce rich and sometimes counterintuitive internal dynamics. Accompanying the zonal wind anomalies of the QBO are anomalies in temperature, upwelling, ozone, and other trace gases.

In 2016, the QBO experienced an unprecedented disruption, shown in Fig. 1 (with each shear zone[1] near the onset of the disruption labeled). The data shown are from the MERRA-2 global atmospheric reanalysis [Gelaro et al. 2017; Global Modeling and Assimilation Office (GMAO); GMAO 2015a]. Prior to the disruption, an easterly shear zone around 10 hPa had been descending into a deep region of westerlies. At the beginning of the disruption, easterly shear zone #2 formed around 40 hPa, splitting the deep westerlies. Subsequently, easterly shear zone #2 descended toward the top of the buffer zone [the region above the tropopause where the QBO vanishes, analyzed in Match and Fueglistaler (2019)]. The easterly shear zone that had been originally descending (shear zone #4) and the upper westerly shear zone #3 both stagnated and gradually ascended. When easterly shear zone #2 reached the buffer zone, it annihilated westerly shear zone #1, and westerly shear zone #3 began descending. When westerly shear zone #3 reached the buffer zone, it annihilated easterly shear zone #2, and easterly shear zone #4 began descending. Easterly shear zone #4 eventually annihilated the stalled shear zone #3. The QBO ultimately recovered to its typical oscillation.

The 2016 disruption appeared to be caused by at least one process external to the typical QBO mechanism. But, it is unclear what confluence of events was necessary to cause the disruption, or how the features of the disruption constrain those processes. To date, several external perturbations have been proposed to cause features of the 2016 disruption. Most reanalysis-based accounts of the 2016 disruption invoke 1) a triggering to form the anomalous easterly shear zone #2. The triggering has been linked to horizontal eddy momentum flux divergence associated with dissipation of planetary waves originating in the Northern Hemisphere midlatitudes (Osprey et al. 2016; Coy et al. 2017; Barton and McCormack 2017; Watanabe et al. 2018; Lin et al. 2019). As a notable exception, Renaud et al. (2019) showed in the 1D QBO model that 2) enhanced total wave stress can drive the QBO into quasi-periodic, frequency-locking, or chaotic regimes, some of which can produce patterns that resemble QBO disruptions without an external triggering. Additional external perturbations invoked to explain aspects of the QBO disruption include 3) increased mean residual upwelling that caused the stagnation of shear zone #4 and ascent of shear zone #3 (Newman et al. 2016), 4) increased secondary residual upwelling associated with the QBO vertical shear that caused the ascent of shear zone #3 (Newman et al. 2016; Coy et al. 2017), and 5) enhanced Kelvin wave stress that permitted shear zone #3 to stagnate (Li et al. 2019).

[1] In QBO literature, "shear zone" conventionally refers to a connected region with the same sign of zonal-mean zonal wind, and not (as might be expected) to a connected region with the same sign of vertical wind shear.

Corresponding author: Aaron Match, amatch@princeton.edu

DOI: 10.1175/JAS-D-20-0172.1

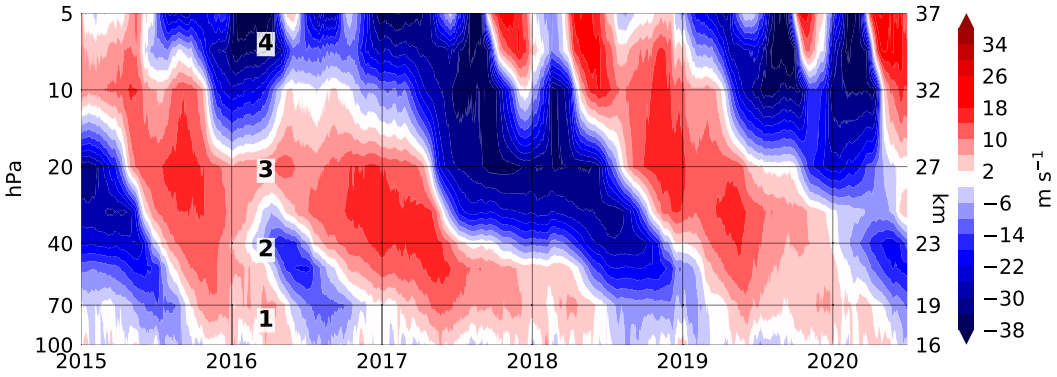

FIG. 1. Monthly averaged MERRA-2, latitudinally averaged 5°S–5°N. The QBO disruption can be seen to begin around 40 hPa in 2016. The right y axis indicates approximate (log-pressure) height $z = H\ln(p_0/p)$ with $H = 7$ km.

The latter three proposed external perturbations seek to explain the occurrence of stagnation and ascent that was unprecedented going back to at least 1953. Yet, given the richness of the internal dynamics of the QBO, it is not clear whether all of these external perturbations are necessary to explain the zonal wind evolution. Different mechanisms can explain the same zonal wind evolution while making different predictions for other aspects of the stratospheric state. For example, if the ascent of shear zones is explained via anomalous upwelling, then that implies unprecedented transport of trace gases during the disruption (as studied in Tweedy et al. 2017). If, on the other hand, the shear zone ascent was due to climatological upwelling, then there need not have been unprecedented transport. Understanding the perturbed dynamics of the QBO during the disruption can improve the constraint provided by the observed wind on the broader stratospheric state.

We seek a minimal prescription of external perturbations required to produce QBO disruptions. Ideally, general circulation models (GCMs) could be used to develop a minimal prescription for the comprehensive three-dimensional evolution of the atmospheric state during the QBO disruption. Yet, of the minority of GCMs that spontaneously produce QBOs, disruptions are so rare that there are only a few in the entire CMIP5 archive (three disruptions in 3000 years of simulations with internally generated QBOs) (see also Osprey et al. 2016). The observed disruptions do not provide enough information to determine whether GCMs accurately represent disruption frequency or substantially underestimate it. Deficiencies in the GCM triggering by horizontal eddy momentum flux divergence are hard to rule out, inhibiting the development of a comprehensive theory for disruptions.

Although uncertainties regarding the triggering remain, the internal dynamics of the QBO have been well characterized for decades by the 1D theory of the QBO (Holton and Lindzen 1972; Plumb 1977). The 1D model of the QBO represents the vertical profile of zonal mean zonal wind in the tropical stratosphere as it is driven by vertically propagating waves that dissipate as a function of the mean flow. The internal dynamics of the 1D model follow a periodic orbit on a stable attractor with no states resembling the disruption.[2] Disrupted behavior can be produced by applying an external perturbation. Within this 1D perspective, the occurrence of the disruption implies the action of at least one mechanism external to the 1D theory. In this paper, we study disruptions using the 1D theory by analyzing its response to prescribed triggering. By prescribing the triggering, the disruption is partitioned into a prescribed portion that is not strongly constrained by theory or GCMs (the triggering) and a resolved portion with a rich theoretical basis.

This manuscript originally focused exclusively on the 2016 disruption. During its final stages of preparation for publication, we learned of an ongoing event that resembles the 2016 disruption, which began in January 2020. The early stages of the 2020 event can be seen in Fig. 1.[3] As during the 2016 disruption, the 2020 event has featured a large triggering that reversed the winds around 40 hPa, leading to stagnation and ascent aloft. Unlike during the 2016 disruption, the triggered shear zone of the 2020 event subsequently fused with the previously descending easterly QBO shear zone, and therefore did not produce four distinct shear zones as during 2016. We show that the 2020 event is consistent with our theory of disruptions, and that whether the triggered shear zone fuses with the previously descending shear zone is primarily determined by the phasing of the triggering.

In section 2, we show that the 1D QBO responds to triggering by reproducing all key features of the 2016 QBO disruption. Perturbed QBO dynamics explain the stagnation and ascent of shear zones without requiring anomalous upwelling or wave stress. Subsequently, the framework developed to interpret the 2016 disruption is applied to the recent 2020 event. The success of the 1D theory at describing the role of internal dynamics during the 2016 disruption and 2020 event highlights shortcomings in understanding when triggering does or does not cause a disruption. In section 3, we show that insights from the 1D theory on triggering are difficult to reconcile with the history of triggering events and responses in MERRA-2.

[2] Possible exceptions in a high wave forcing regime, as in Renaud et al. (2019) are discussed in section 2d.

[3] Our original arguments about the 2016 disruption were based on data that extended until November 2018. After learning of the 2020 event, our dataset along with Fig. 1 was extended to the most recent available data, July 2020.

We raise concerns about the reliability of the MERRA-2 resolved momentum budget during the 2016 disruption.

2. Perturbed dynamics of the QBO

In this section, the 1D theory of the QBO is introduced. Relevant principles from the 1D theory are applied to explain key features of QBO disruptions. The stagnation and ascent of shear zones above 40 hPa are explained as perturbed dynamics in response to a triggering.

a. Introduction to 1D theory

The 1D theory of the QBO represents the tropical stratosphere as a column driven by interactions between the mean flow and vertically propagating waves that originate at the lower boundary (Holton and Lindzen 1972; Plumb 1977). Our treatment of wave dissipation follows Plumb (1977), which assumed two vertically propagating gravity waves with zonal phase speeds c and $-c$ that propagate rapidly relative to the evolution of the mean flow. Our implementation of the 1D model is described in the appendix. The amplification of mean flow anomalies by dissipation of vertically propagating waves can be understood by considering two key principles from linear wave dynamics. First, when a wave dissipates, it accelerates the wind toward its phase speed. Second, the vertical group velocity of a vertically propagating gravity wave depends nonlinearly on the mean flow as $c_{gz} = k(\overline{u} - c)^2/N$, with wavenumber k, background zonal wind $\overline{u}$, phase speed c, and buoyancy frequency N. The dispersion relation shows that a wave propagates upward more slowly when the zonal wind is close to its phase speed. If the wave dissipates at a constant rate in time, then the more slowly it ascends, the more dissipation occurs per unit height. The acceleration toward the wave's phase speed grows stronger as the wind approaches the wave's phase speed, which amplifies wind anomalies.

Figure 2 illustrates a sample wave drag calculation for a sinusoidal zonal wind profile. The wind profile has westerlies in the lower half of the domain, maximizing at 22 km, and easterlies in the upper half of the domain, maximizing at 32 km. The westerly wave ($c = 30\,\mathrm{m\,s^{-1}}$) dissipates at the lower westerly wind maximum, so it is *shielded* from influencing the winds aloft. Above 22 km, the net wave drag is consequently easterly until reaching the easterly wind maximum at 32 km, where the easterly wave also dissipates.

The 1D model with n vertical levels contains $n - 2$ degrees of freedom. (Each boundary condition contains no independent information.) The 1D QBO occupies a phase space with $n - 2$ dimensions. The unperturbed evolution of the QBO resides on a stable attractor within this phase space. The stable attractor typically has two shear zones in the domain at any given time. The lower shear zone is stalled at the bottom of the domain. The upper shear zone is descending from the top of the domain on a course to annihilate the stalled shear zone. The winds above the upper shear zone are shielded. The system evolves so when the upper shear zone annihilates the stalled shear zone, it becomes the new stalled shear zone, and a shear zone matching the sign of the annihilated shear zone reforms at the top of the domain.

Various strategies have been used to reduce the dimensionality of the QBO, exploiting its large vertical scales and periodicity. Wallace et al. (1993) showed that 95% of the variance of the QBO can be captured in two dimensions by the leading two empirical orthogonal functions (EOFs) of tropical stratospheric zonal mean zonal wind from 70 to 10 hPa. The principal components of those leading two EOFs vary in quadrature, and can be further reduced into a one-dimensional metric of QBO phase. These dimensionality reductions are effective at capturing the QBO evolution on the stable attractor or in the presence of small-amplitude noise. However, the multidimensionality of the QBO cannot be denied during a disruption, when these traditional dimensionality reductions fail to capture its evolution. During a disruption, the typically rigid phase relationships among vertical levels are reconfigured, projecting less strongly onto the climatological EOFs. Tweedy et al. (2017) mentioned that during the 2016 disruption, the two leading EOFs only captured 71% of the variance, the lowest fraction of variance captured by these EOFs during the period 1987–2017. A theory for disruptions must retain dimensionality greater than two so that it can represent QBO dynamics when the phase relationships among levels have been reconfigured.

Because the 1D theory includes significant simplifications, it produces at most a qualitative theory for QBO disruptions.[4]

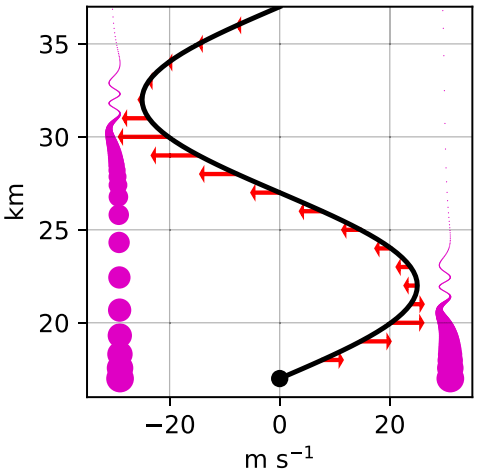

FIG. 2. Sample wave drag calculation as in Plumb (1977). Zonal wind is sinusoidal with amplitude 25 $\mathrm{m\,s^{-1}}$ (black). Wave momentum flux of vertically propagating waves (magenta circles) is centered over wave phase speed ($\pm 30\,\mathrm{m\,s^{-1}}$), the area of each circle is proportional to the wave momentum flux reaching that level (with a minimum size cutoff), the circles are placed once per day, the low-period horizontal oscillation in the magenta indicates the passage of time with a period of 60 days. The vertical derivative of circle area is the vertical wave momentum flux divergence for each wave, which when divided by density and summed for both waves equals the total wave drag (red arrows). The full 1D model is documented in the appendix.

[4] Simplifying assumptions in the 1D theory include the following: the 1D QBO is driven by only two waves rather than a spectrum, those waves are only gravity waves rather than a diverse family of tropical waves, there is no horizontal momentum flux divergence, no secondary meridional upwelling associated with the QBO, no zonal asymmetries or latitudinal structure, the wave source is stationary and symmetric about zero, there is a zero-wind lower boundary condition, and there is unrealistically large vertical diffusivity arguably serving as a proxy for localized shear instabilities.

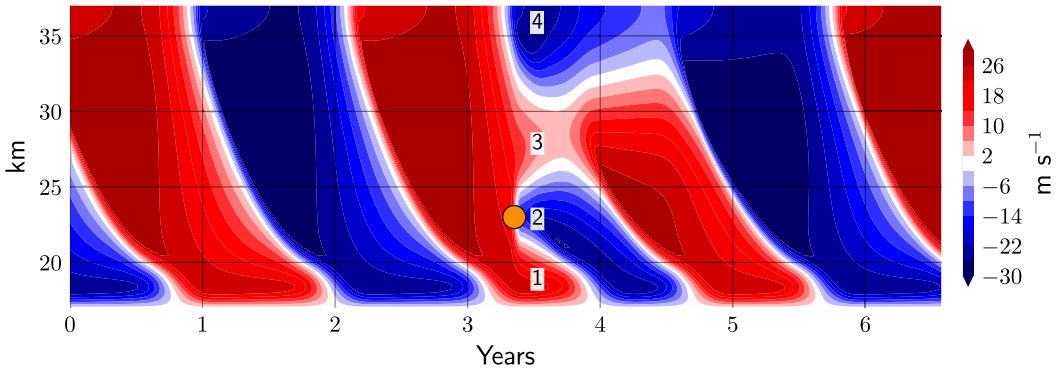

FIG. 3. One-dimensional model simulation configured as in Plumb (1977). A triggering is imposed at the orange marker leading to a disruption qualitatively similar to the observed disruption. The triggering is a prescribed acceleration with peak amplitude -2×10^{-5} m s^{-2} Gaussian in height centered at 23 km with decay scale 2 km, and is half sinusoidal in time across 30 days. The full 1D model is documented in the appendix.

Its simplicity permits easy interpretation of the perturbed QBO dynamics and lights the way toward addressing open problems.

b. 1D theory of disruptions

We now consider the 1D theory for QBO disruptions. We focus on which features of the 2016 disruption can be explained by the perturbed dynamics in response to the triggering. First, the 1D model of the QBO is considered without upwelling, which predicts that wave shielding causes shear zones to stagnate above 40 hPa, as observed during the 2016 disruption. The 1D model can be emulated by a heuristic dynamical model of the perturbed QBO, which facilitates easy interpretation of the shear zone stagnation. Second, climatological (constant) upwelling is included in the 1D model, which predicts that the stagnant shear zones above 40 hPa will ascend, as was also observed. The agreement between the 1D model and the 2016 disruption suggests that stagnation and ascent result from the joint effects of wave shielding and climatological upwelling.

1) WAVE SHIELDING CAUSES STAGNATION

Triggering perturbs the QBO from its stable attractor, reconfiguring the phase relationships among levels. Triggering can create a situation with four shear zones as opposed to the typical two. The lowest two of those four shear zones shield the region above the triggering from wave drag, causing the winds above the triggering to stagnate. These results are shown first in the 1D model of the QBO, then in a heuristic dynamical model that emulates the 1D model and facilitates a simple geometric interpretation of disruptions.

(i) 1D model

Figure 3 shows an idealized disruption in the 1D model without upwelling. The idealized disruption is caused by a single external perturbation, a triggering that is localized in space (Gaussian with decay scale 2 km) and time (half sine with duration 30 days), which forms an easterly shear zone within a stalled westerly shear zone. The simulated disruption resembles the 2016 disruption from Fig. 1. Following the formation of the triggered shear zone #2 at 23 km, the winds above 23 km stagnate in a manner similar to what was seen in 2016. The winds ascend slightly as a result of diffusion in the model, but we show later that the ascent of the stagnant shear zones is best understood to result from climatological upwelling.

(ii) Heuristic disruption: Stagnation

The 1D theory can be emulated by 1D heuristics, which provide a simple geometric framework for perturbed QBO dynamics. Consider the following heuristics, designed as a dynamical rule set for intuitively emulating the 1D model:

- The lowest shear zone is stalled at the lower boundary.
- The second lowest shear zone (opposite in sign to the lowest shear zone) is descending at a constant rate w on a course to annihilate the lowest shear zone.
- Together, the two lowest shear zones dissipate all of the wave momentum flux, shielding the winds above them.
- If a wave reaches the upper boundary, it instantaneously forms a new shear zone there.

With these heuristics alone, the stable QBO *and perturbations therefrom* can be emulated. A generic disruption can be constructed that qualitatively matches the disruption in the 1D model and observations. Due to simplifying assumptions, the 1D heuristics should not be considered a quantitative substitute for the 1D model.[5] The 1D heuristics do provide an interpretive framework that focuses attention on the key dynamics of the 1D model of relevance for problems like QBO disruptions. The 1D heuristics bear some resemblance to previously formulated descent rate models of the QBO, but in contrast to those previous works, we elicit the dynamics of multiple shear zones by considering wave shielding while assuming a constant descent rate for unshielded shear zones (e.g., Dunkerton 2000; Rajendran et al. 2018; Match and Fueglistaler 2020).

[5] Some of the simplifying assumptions when moving from the 1D theory to the 1D heuristics include the following: only the sign but not the magnitude of shear zones determines their dissipation characteristics, dissipation is complete in the lowest shear zone that matches the wave's phase speed, descent rate is constant, reformation of a shear zone aloft is instantaneous, and vertical diffusion is neglected except for its contribution to the constant descent rate.

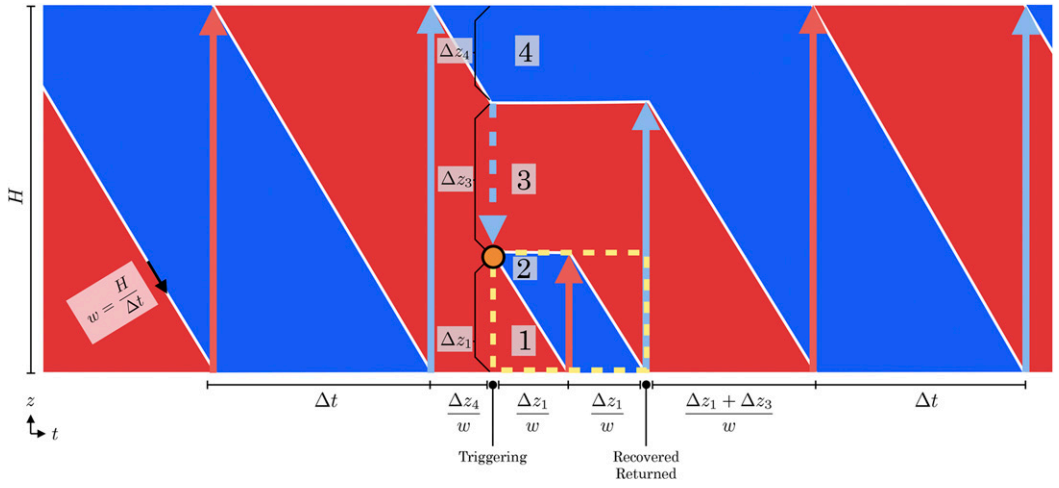

FIG. 4. Heuristic disruption with zero upwelling based on heuristics in section 2b(ii). When a stalled shear zone is annihilated, wave momentum flux matching its sign transmits into the domain (blue arrows indicate easterly wave momentum flux, red arrows indicate westerly wave momentum flux). Typically, the heuristic QBO only ever produces two shear zones. The triggering (orange marker) forms an easterly shear zone #2, after which the remaining features of the disruption follow based on the heuristic dynamics of the perturbed QBO. Shear zone labels and depths are defined immediately after the triggering, with the ith shear zone above the buffer zone having depth Δz_i. Following the triggering, the dissipation level of the easterly wave shifts downward from shear zone #4 to shear zone #2 (dotted blue arrow). Note that the dissipation level shifts downward but the wave momentum flux only ever propagates upward. The disruption contains a miniature QBO subcycle (yellow box). The QBO recovers to the stable attractor and returns to its pretriggering state at the same time, meaning the disruption is cyclic.

Figure 4 shows a generic QBO disruption constructed by application of the 1D heuristics. Immediately prior to the disruption, a westerly shear zone is stalled at the lower boundary. The stalled westerly shear zone dissipates the westerly wave, shielding the rest of the domain from westerly wave drag. The easterly wave propagates upward to the descending easterly shear zone, which has a depth of Δz_4 below the top of the domain. The disruption is initiated by a triggering, which reverses the wind to easterly at height Δz_1 above the lower boundary. The easterly wave that previously would have reached the original easterly shear zone #4 at height $\Delta z_1 + \Delta z_3$ now dissipates on the triggered shear zone #2 at Δz_1. The triggered easterly shear zone #2 immediately begins descending, while the original easterly shear zone #4 stagnates. The original westerly shear zone has been split in two by the new easterly shear zone. The lower branch of the original westerly shear zone #1 remains stalled, shielding the upper westerly shear zone #3 and causing it to stagnate.

The triggered easterly shear zone #2 deepens with time because the top stagnates while the bottom descends. Eventually, the triggered easterly shear zone #2 annihilates the stalled westerlies (shear zone #1), which occurs after a time equal to the depth of shear zone #1 divided by the QBO descent rate ($\Delta z_1/w$). When the stalled westerly shear zone #1 is annihilated, the westerly wave is now transmitted to the upper branch of the split westerly shear zone (3). There, the westerly wave dissipates and the westerly shear zone #3 begins descending. As the westerly shear zone descends, it reverts the triggered easterlies back to westerlies. The triggered easterlies endure at any given level for time $\Delta z_1/w$. The descending westerlies from shear zone #3 annihilate the stalled easterly shear zone after descending for a time of $\Delta z_1/w$. The triggered easterly shear zone endures for a total time of $2\Delta z_1/w$.

Once the triggered easterlies are annihilated, there are only two shear zones in the domain. In the heuristic dynamical model, any configuration with two shear zones is on the stable attractor. Therefore, the QBO has recovered to the stable attractor. When the QBO recovers to the stable attractor, something special has occurred: at the exact time of recovery, the winds exactly match the state immediately prior to the triggering. The time when the winds exactly match the state immediately prior to the triggering is the *return*. If the QBO recovered to a random location on the stable attractor, then the return would be expected to occur an average of half the QBO period afterward. Because the recovery and return occur at the same time, the QBO disruption is cyclic, and can be conceptualized as a cyclic "wrinkle" in the QBO progression. Below the triggering level, the QBO undergoes a full subcycle with descending easterlies followed by descending westerlies. Both of these shear zones begin descending from height Δz_1, and the typical QBO dynamics play out in miniature as if there was an upper boundary condition at height Δz_1 rather than the typical H. Above the triggering level, the QBO stagnates during the entire disruption.

The 1D heuristics suggest a powerful constraint on disruptions: to produce a shear zone that immediately amplifies and descends, triggering must reverse the sign of the wind in the stalled shear zone. If the triggering did not reverse the wind, then it would not modify the wave shielding. If the triggering

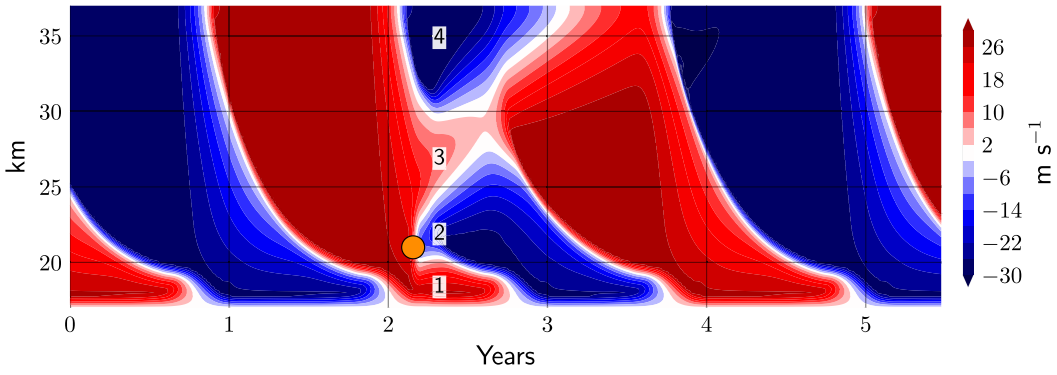

FIG. 5. One-dimensional model simulation as in Fig. 3, but with constant upwelling of 0.2 mm s^{-1}, $F_L = 0.016\ m^2\ s^{-2}$, and the triggering centered at 22 km. The full 1D model is documented in the appendix.

reversed the wind, but did so above the stalled shear zone, then the triggered shear zone would be shielded and would stagnate.

2) Climatological upwelling displaces stagnant shear zones upward

Wave shielding causes stagnation. Without mean upwelling, a stagnant wind anomaly is in static equilibrium on a fixed vertical level. With mean upwelling, a stagnant wind anomaly will be advected upward on a material surface. Therefore, stagnation in the presence of climatological upwelling can explain shear zone ascent without invoking anomalous transport.

(i) 1D model with upwelling

Figure 5 shows the perturbed 1D dynamics of the QBO with climatological upwelling. The base state QBO now must overcome the resistive effects of upwelling in order to descend (McIntyre 1994; Match and Fueglistaler 2020). To maintain a reasonable QBO period, the wave stress at the lower boundary is increased from 0.01 $m^2\ s^{-2}$ in the nonupwelling experiment to 0.016 $m^2\ s^{-2}$ in the upwelling experiment. When there is climatological upwelling, stagnant shear zones ascend. The easterly shear zone that was originally descending (shear zone #4) ascends out of the domain. The upper westerly shear zone #3 ascends as long as it remains shielded. The triggered easterly shear zone grows downward due to wave-driven descent and upward due to upwelling. It does not stop growing upward until the westerly shear zone above it begins descending.

(ii) Heuristic disruption: Ascent

The heuristic disruption of the 1D theory can be modified to include the effects of upwelling. Based on the 1D simulation in Fig. 5, the following rule can be added to the heuristic simplification of the 1D theory: stagnant shear zones ascend at the climatological upwelling speed. For simplicity, the following analysis assumes that the climatological upwelling speed equals the climatological QBO descent rate (which is the total descent rate accounting for wave dissipation, diffusion, and upwelling), and both speeds are referred to as w. The ascent of stagnant shear zones does not affect the dynamics on the stable attractor. This is consistent with the fact that shear zone ascent during the 2016 disruption was unprecedented; the internal dynamics of the QBO on its stable attractor never produce situations in which a stagnant shear zone ascends.

With climatological upwelling, the conceptual understanding of disruptions must be modified. Figure 6 shows a heuristic disruption with upwelling that matches the key features of the 1D disruption with upwelling in Fig. 5. The disruption shown in Fig. 6 is just one of several possible regimes, which depend on the relationship between the height of the original easterly shear zone below the upper boundary, Δz_4, and the height of the triggering, Δz_1. The disruptions are not periodic (the return time is longer than the recovery time), and the expressions for recovery time and return time depend on the regime. The case in Fig. 6 depicts the QBO recovering when shear zone #4 exits the top of the domain, which is only true if $3\Delta z_1 > \Delta z_4 > \Delta z_1$. The recovery time is $\Delta z_4/w$. The return time is $(\Delta z_4 + 3\Delta z_1)/w$.

The disruption can end with other conditions, depending on the relative depths of the shear zones at the beginning of the triggering. If the bottom shear zone is larger than the top shear zone ($\Delta z_1 > \Delta z_4$), then the recovery occurs when shear zone #1 is annihilated, which occurs $\Delta z_1/w$ after the triggering. The return time is still $(\Delta z_4 + 3\Delta z_1)/w$. If the upper shear zone is more than 3 times larger than the bottom shear zone ($\Delta z_4 > 3\Delta z_1$), then shear zone #4 does not have time to exit the top of the domain before the QBO recovers. Instead, shear zone #2 is annihilated after $3\Delta z_1/w$, at which time the QBO has recovered and shear zone #4 begins descending. In this case, the return time is $6\Delta z_1/w$.

By having an upper boundary, the model truncates dynamics that would otherwise play out according to its heuristics above the domain of representation. It raises the question of what sets the top of the QBO, and how the dynamics of the QBO transition into the dynamics aloft, which are dominated by the semiannual oscillation (SAO). How this transition region is characterized could determine whether the original easterly shear zone #4 is considered to exit the QBO domain in the observations or whether it remains in the QBO domain. Because realistic wave dynamics do not respect arbitrary truncations in height, it seems clear that in early 2017, shear zone #4 is part of the QBO (Fig. 1). One interpretation of the transition region between the QBO and SAO suggested by this work is that the SAO is typically shielded from the waves participating in the QBO, so that it is stagnant from the perspective of the QBO. Indeed, the SAO is believed to be driven

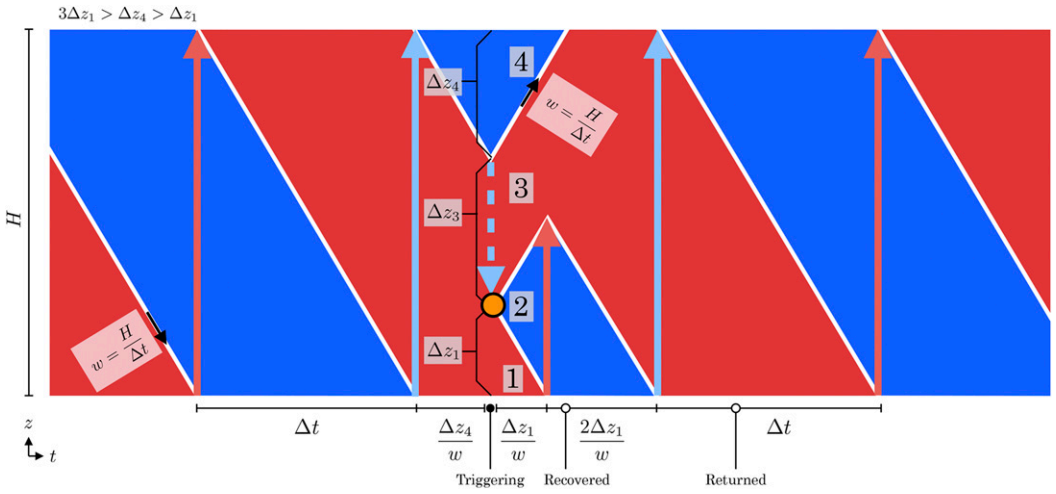

FIG. 6. Heuristic disruption as in Fig. 4, but with upwelling w (for simplicity, assumed equal and opposite to the total QBO descent rate). The QBO recovers when shear zone #4 exits through the top of the domain after a time of $\Delta z_4/w$, although return to the pretriggering state occurs substantially later after $(\Delta z_4 + 3\Delta z_1)/w$. Timeline labels refer to the duration between breakpoints, which are represented by vertical bars or closed circles, but not by open circles. The case shown is when $3\Delta z_1 > \Delta z_4 > \Delta z_1$. Other expressions for timing, recovery, and return apply when $\Delta z_4 > 3\Delta z_1$ or $\Delta z_1 > \Delta z_4$.

by waves with phase speeds outside the zonal mean zonal wind envelope of the QBO. Following the annihilation of a stalled shear zone, an SAO shear zone can become unshielded, in which case it might adopt blended characteristics of the SAO and QBO. An SAO shear zone that is unshielded from the perspective of the QBO could help form the seed of a new QBO shear zone (e.g., Lindzen and Holton 1968; Dunkerton and Delisi 1997).

c. *Phase dependence of triggering and the 2020 event*

In this subsection, we apply the 1D theory developed based on the 2016 disruption to the 2020 event. Note that we only use ideas and simulations that predated our knowledge of the 2020 event.

Whereas the 2016 disruption featured a disconnected easterly shear zone formed via triggering at 40 hPa, the 2020 event featured an easterly shear zone formed via triggering at 40 hPa that subsequently fused with the previously descending easterly shear zone, giving a visual impression more typical of the unperturbed QBO (Fig. 1). Given its connected nature, it is arguable whether the 2020 event should be considered a disruption. On the one hand, the 2020 event featured a large triggering that reversed the winds at 40 hPa, forming a shear zone that ultimately descended. On the other hand, the reversed winds fused with a shear zone aloft. Setting aside definitional questions, we demonstrate that events resembling the 2020 event are consistent with the 1D theory, emphasizing the phase-dependent response of the QBO to triggering.

If triggering is applied in the 1D model soon before the descending easterly shear zone would have reached the triggering level anyway, then the triggered shear zone can become connected to the previously descending shear zone. Figure 7 shows 1D model experiments in which the triggering ends 90 days before the easterly shear zone would have reached the triggering level. In cases with or without upwelling, the 1D model fuses the triggered shear zone with the previously descending shear zone. Note that the triggering amplitude in Fig. 7 matches that of the previous 1D disruption experiments (Figs. 3 and 5); it is only the phasing that has changed. The 1D model reproduces the fusing of the two easterly shear zones.

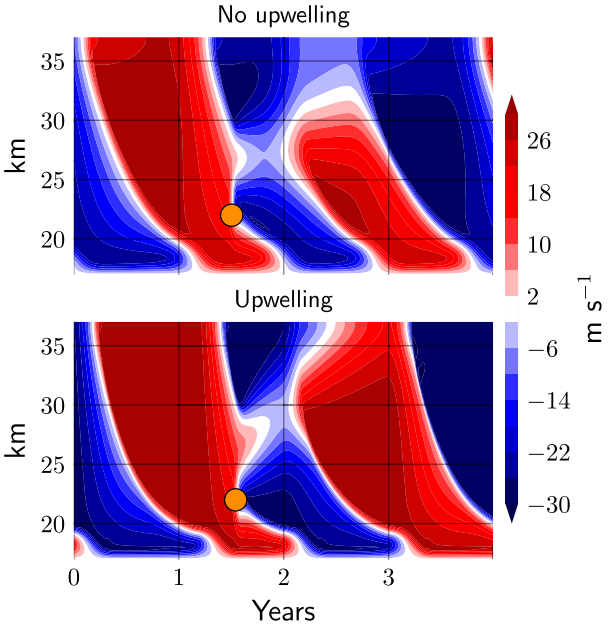

FIG. 7. One-dimensional model experiments resembling the 2020 event (Fig. 1), but with the triggering prescribed to occur 90 days before the descending easterlies would have reached the triggering level. Other than the modified phasing of the triggering, the 1D model configurations match previous cases analyzed (top) with no upwelling (compare to Fig. 3) and (bottom) with upwelling (compare to Fig. 5). The full 1D model is documented in the appendix.

The fusing of the easterly shear zones is understood to result from vertical diffusion that annihilates the stagnant westerlies. An imprint of the stagnant westerlies remains even after they are annihilated by diffusion, in the form of a region of weak easterly winds above the triggering. The easterly winds above the triggering can remain weak because they never form a critical layer to the easterly waves; the easterly critical layer skips down from the previously descending easterly shear zone to the triggering level (as in the heuristic model described previously in this section, e.g., Fig. 4). These weak easterlies are more susceptible to westerly wave dissipation, thereby forming the seed for a new westerly shear zone once the stalled westerly shear zone is annihilated early in year 2 of the 1D simulations (Fig. 7). The MERRA-2 assimilation of the 2020 event provides an early hint of such reformation of the westerlies at and above the triggering level (Fig. 1).

Despite the visual differences between the 2016 disruption with its disconnected shear zone and the 2020 event with its connected shear zones (Fig. 1), the 1D framework suggests no fundamental distinction between these two events. Measures of connectedness assume a sharp dynamical threshold between the dynamics of westerly winds and easterly winds, separated by a critical wind speed of 0 m s^{-1}. Because wave dissipation of the QBO actually varies continuously with respect to wind speed in the vicinity of zero wind, the differing connectedness of the 2016 disruption versus the 2020 event does not constitute a significant dynamical distinction. Indeed, the simulated 2016-like disruption and the 2020-like event have strong dynamical similarities, which stem from the dynamically similar behavior of stagnant weak easterly winds and stagnant weak westerly winds in the QBO region. For example, the reformed midlevel westerly shear zones in the 2020-like simulation (Fig. 7) strongly resemble the reformed midlevel westerly shear zones 3 in the 2016-like simulation (Figs. 3 and 5).

d. *Evaluating which external perturbations were necessary for the 2016 disruption*

The success of the minimal model at reproducing the key features of the 2016 disruption and 2020 event means that stagnation and ascent do not necessarily imply anomalous upwelling or Kelvin wave stress. That the key features of the 2016 disruption match a disruption caused by only triggering suggests that the other proposed external perturbations were weak or absent. To argue that such external perturbations nonetheless occurred, independent evidence other than the qualitative features of the wind evolution must be provided. We briefly return to each of the external perturbations hypothesized to act during the 2016 disruption, covering the evidence for them and how our results impact the case for their role during the 2016 disruption. Where relevant, we comment on whether MERRA-2 diagnostics support our argument. Triggering, the only essential external perturbation, is covered in the next section.

The unprecedented ascent of westerly shear zone #3 from 20 to above 10 hPa during the 2016 disruption has been hypothesized to result from 1) anomalous residual upwelling, and, more specifically, 2) anomalous secondary residual upwelling (Newman et al. 2016; Coy et al. 2017). If anomalous upwelling was necessary to explain the anomalous shear zone ascent, then the observed shear zone ascent would imply anomalous tracer transport. Section 2b showed that an ascending stagnant shear zone neither requires nor implies anomalous upwelling; it merely requires that the total upwelling, including the climatological component, be positive. We investigate MERRA-2 for evidence of unprecedented upwelling during the 2016 disruption. At 10 hPa, the level to which shear zone #3 ascended during the 2016 disruption, the climatological (time-averaged) residual upwelling averaged from 5°S to 5°N is 0.4 mm s^{-1}, with an annual cycle (in the monthly average) between 0 and 0.9 mm s^{-1}. The total monthly residual upwelling at 10 hPa was positive throughout the 2016 disruption, peaking in February at 1.3 mm s^{-1}, which ranks eighth in the MERRA-2 record. Secondary upwelling, calculated as the component of MERRA-2 deseasonalized upwelling that varies linearly with the MERRA-2 deseasonalized vertical wind shear ($r^2 = 0.6$), peaked in April and May at 0.6 mm s^{-1}, ranking sixth and seventh in the MERRA-2 record. The disruption clearly included some months with large positive anomalies in upwelling. Yet the total and secondary upwelling anomalies diagnosed during the disruption are each eclipsed by at least five events that did not cause shear zone ascent. Thus, the MERRA-2 data do not suggest a need to revise the theoretical result that stagnation along with climatological mean upwelling is sufficient to explain the observed shear zone ascent. Note that rather than causing the anomalous ascent, modest anomalies in upwelling (and transport) can be thought of as resulting from the disruption, in connection with the stagnation and ascent of secondary upwelling features that would typically descend.

It has been argued that the stagnation of westerly shear zone #3 was enhanced by anomalous Kelvin wave stress during El Niño of 2015/16 (Li et al. 2019). Our results indicate that there need not have been unprecedented Kelvin wave stress to explain the stagnation, which resulted instead from wave shielding. It is plausible that there was enhanced Kelvin wave stress during the winter 2015/16 associated with El Niño, but it is not required to explain the stagnation.

Renaud et al. (2019) showed that increasing a 1D model parameter related to the wave stress could shift the QBO to a regime with internally generated disruptions (no triggering required). Their results suggested that a transient increase in wave stress, such as might have occurred during the 2015/16 El Niño, could potentially shift the QBO into a regime with internally generated disruptions. It is not clear whether internal variability in wave stress is large enough to cause a QBO regime change. Beginning with the 1D QBO configuration used in this paper, which has a period matching the observed value of 800 days without producing excessive shears, the QBO wave stress must be increased by greater than a factor 8 in order to exit the period 1 regime. Before exiting the period 1 regime, the increased wave stress shortened the QBO period to 150 days. These tests suggest that the internally generated disruptions described in Renaud et al. (2019) might represent exotic QBO regimes that are far from the observed state. More work is needed to clarify potential analogies between the theoretical results of Renaud et al. (2019) and the observed QBO.

Our results indicate that the stagnation and ascent of shear zones during the 2016 disruption can be accounted for by the

QBO response to triggering with climatological upwelling. There is no need to invoke anomalous upwelling or wave stress to reproduce the key features of the 2016 disruption.

3. The triggering of QBO disruptions

The 1D theory provides a coherent explanation of stagnation and ascent. This qualitative theory for QBO disruptions reduces the number of external perturbations needed to cause the QBO disruption down to one: triggering. Given the fundamental role played by triggering during disruptions, in the following we investigate the triggering in the 1D theory. We show that the 1D theory does not provide a quantitative framework for understanding when triggering does or does not lead to disruptions. Such a framework would need to distinguish past *nondisruptive* triggering from the 2016 disruptive triggering and the 2020 triggering. In this section, we briefly survey the landscape of understanding of triggering.

In the heuristic theory for QBO disruptions, only the sign of the wind matters and not its magnitude. This simplification suggests that a triggering is disruptive if and only if it reverses the sign of the wind. The importance of reversing the sign of the wind suggests a sharp threshold near zero in the response to triggering. Yet such a sharp threshold does not occur in the full 1D model, in which the magnitude of the wind matters and which responds continuously to changes in triggering magnitude. The heuristic theory for QBO disruptions also suggests that triggering produces an amplifying and descending disruption only when applied in the lowest shear zone. This prediction is supported by the full 1D model, meaning that the response to triggering depends strongly on the QBO phase when it is applied.

Putting these pieces together, the 1D theory predicts that similar triggering magnitudes during similar QBO phases should lead to similar perturbed QBO responses. This expectation conflicts with results from the reanalysis record. The MERRA-2 record has several large triggering events that occurred within stalled westerly shear zones (as in 2016), but did not lead to disruptions (GMAO 2015a,b). Figure 8 shows histograms of the horizontal eddy momentum flux divergence along with histograms of other key terms in the momentum budget, comparing the 2016 disruption and 2020 event with all other times in the record. Easterly triggering events appear on the left side of the distribution of horizontal eddy momentum flux divergence. The triggering during the 2016 disruption was the largest on record. Had the triggering acted alone, the wind would have accelerated $-11.5\,\mathrm{m\,s^{-1}}$ at 40 hPa in the 120-day period ending 4 April 2016, at the end of the peak triggering during the 2016 disruption. The second-largest triggering occurred during the 2020 event, during which the triggering alone would have accelerated the wind $-9.5\,\mathrm{m\,s^{-1}}$ at 40 hPa in the 120-day period ending 6 October 2019.[6] Yet there is a continuous spectrum of triggering in Fig. 8, including large triggering events that did not disrupt the QBO. The third-largest triggering on record occurred during a similar QBO phase as the 2016 triggering. This nondisruptive triggering would have accelerated the wind by $-9.4\,\mathrm{m\,s^{-1}}$ during the 120-day period ending 7 March 1988, which is nearly identical to the 2020 triggering and only 20% weaker than the 2016 triggering. No disruption occurred in 1988, and the wind actually decelerated less during the triggering period than if the triggering had acted alone. Large nondisruptive triggering, such as in 1988, cannot be reconciled with the 1D theory.

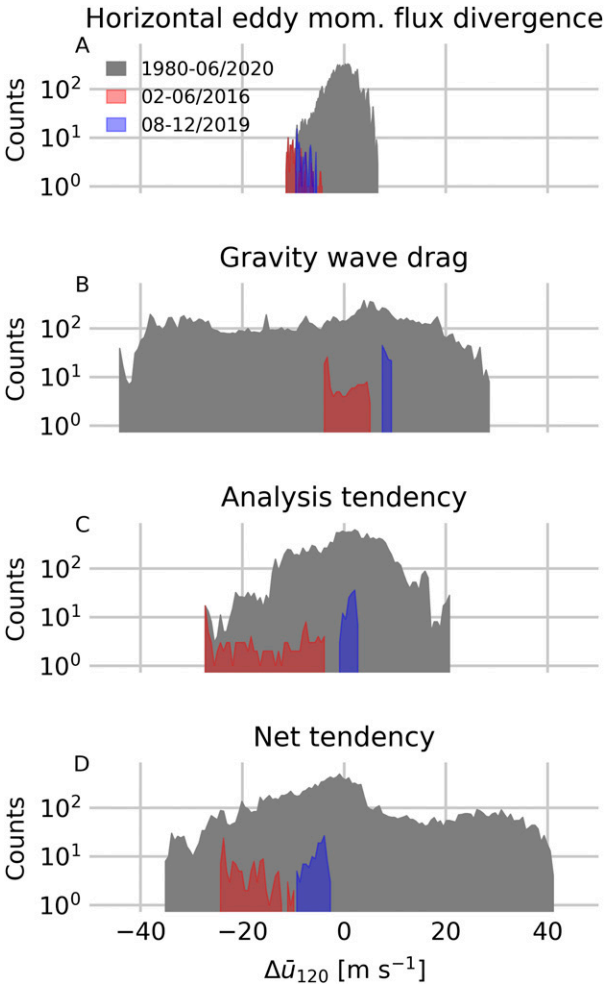

FIG. 8. Histograms of 120-day rolling sums of acceleration due to single terms in the momentum budget of the tropical stratosphere at 40 hPa from 5°S to 5°N in MERRA-2. The gray shading covers the entire time period of 1 Jan 1980 to 30 Jul 2020, red shading highlights the 2016 triggering (1 Feb to 1 Jul 2016) peaking at $-11.5\,\mathrm{m\,s^{-1}}$, and blue shading highlights the 2020 triggering (1 Aug to 1 Dec 2019) peaking at $-9.5\,\mathrm{m\,s^{-1}}$. Horizontal eddy momentum flux divergence represents the triggering.

The range of values of the horizontal eddy momentum flux divergence (Fig. 8a) is small compared to that of the gravity wave drag (Fig. 8b) or net tendency of the wind (Fig. 8d). During the 2016 disruption, the gravity wave drag and net tendency of the wind did not exhibit unprecedented behavior. The only term other than the horizontal eddy momentum flux divergence that exhibited record-breaking values was the

[6] The triggering that caused the 2020 event will be referred to as the "2020 triggering," although it maximized in 2019.

analysis tendency. The analysis tendency is applied within the data assimilation framework so that the general circulation model underlying MERRA-2 can reflect the constraints provided by observations. When the analysis tendency is zero, it indicates that the self-consistent evolution of the model adheres to the constraints from observations. When the analysis tendency is large, it indicates that large deviations from self-consistency are necessary for the model to resemble the observed evolution. In the 120-day period ending 21 May 2016, the analysis tendency alone would have accelerated the wind by $-27.3\,\mathrm{m\,s^{-1}}$, the largest easterly acceleration due to the analysis tendency on record and more than twice the triggering implicated in causing the 2016 disruption. The large analysis tendency indicates that large accelerations during the 2016 disruption are missing from the resolved momentum budget. Two possible interpretations for the large analysis tendency could be 1) that the easterly triggering was much larger in reality than in MERRA-2, which could modify the conclusions about the magnitude of triggering necessary to cause a disruption and could require reconciliation with the 2020 event, and/or 2) that vertically propagating waves (resolved or parameterized) amplified the triggered easterly shear zone more strongly in reality than in MERRA-2, which opens the possibility that the disruption might inform future improvements in the MERRA-2 wave driving. There could be other interpretations for the record-large analysis tendency. In any case, care should be taken when interpreting the disruption based on the resolved momentum budget alone.

4. Conclusions

The 2016 disruption to the QBO featured an unprecedented evolution of the winds. An easterly shear zone formed where westerlies were expected for the first time on record. Shear zones above the new easterly shear zone stagnated and ascended. A similar event occurred in 2020, in which triggering formed an easterly shear zone, although that shear zone appeared connected to the previously descending easterly zone.

Several external perturbations have been invoked to explain the anomalous behavior of the 2016 disruption, including triggering by horizontal momentum flux divergence, increased mean upwelling, increased secondary upwelling, and enhanced wave stress. Our results using the 1D theory show that the key features of disruptions require only one external cause: triggering. The triggering formed the easterly shear zone. Once formed, the internal dynamics of the QBO combined with the climatological upwelling in the tropical stratosphere are sufficient to explain the key features of disruptions. The stagnation of shear zones resulted from wave shielding by the stalled westerly shear zone at the bottom of the domain and the triggered easterly shear zone, which protected the upper two shear zones from wave-driven descent. The ascent of shear zones above the triggering likely resulted from climatological upwelling acting on the stagnant shear zones, which had no wave-driven descent tendencies to oppose the upwelling tendencies. The 1D theory of the QBO has proven to be a powerful tool for evaluating how strongly the wind anomalies during disruptions constrain other anomalous dynamics.

Because the key features of the 2016 disruption and ongoing 2020 event can be explained by only the triggering and the resulting dynamics of the perturbed QBO, a minimal prescription for these events does not need to include anomalies in upwelling or wave stress. Such anomalies could have occurred, but would need to be explained despite these events' reproducibility without such anomalies. The key to the disrupted environment was the reconfigured phase relationships among different vertical levels, which led to unprecedented wave shielding in the shear zones above the triggering level. The QBO recovered by its typical internal dynamics acting on the anomalous wind profiles, ultimately restoring its preferred state of two shear zones in the domain at the end of 2016, when the triggered easterly shear zone was annihilated.

The 1D theory predicts that phasing is key to the response to triggering. Triggering only forms an amplifying and descending shear zone when it occurs in the lowest shear zone, as occurred in 2016 and 2020. Consistent with the key role played by phasing, the ongoing 2020 event can be understood to result from a triggering that occurred soon before the descending easterly shear zone would have reached the triggering level. The triggered shear zone remains disconnected from the previously descending shear zone when there is sufficient height separation between the previously descending shear zone and the triggering level, as occurred in 2016 but not in 2020.

The 1D theory predicts that wave dissipation in the perturbed QBO varies continuously with the magnitude of the triggering. Therefore, the 1D theory cannot reconcile why triggering events of comparable magnitude and phasing to that which occurred in 2016 and 2020 did not lead to disruptions. One source of uncertainty turns out to be the MERRA-2 record itself. The MERRA-2 account of the 2016 disruption has record-large analysis tendencies, indicating that the reanalysis was struggling to resolve the dynamics. The large analysis tendencies decrease the expected reliability of the resolved momentum budget during the disruption.

Acknowledgments. We thank three anonymous reviewers for their constructive reviews.

Data availability statement. MERRA-2 data used during this study are openly available from the NASA Global Modeling and Assimilation Office's Data and Information Services Center at doi:10.5067/CWV0G3PPPWFW and doi:10.5067/QBZ6MG944HW0.

APPENDIX

1D model

The QBO is driven by vertically propagating waves that interact with the mean flow. One-dimensional models (in altitude) are the minimal configurations that represent these wave–mean flow interactions, and these models facilitate understanding of the base state QBO and its response to dynamical perturbations. We analyze the following 1D model of the QBO:

$$\frac{\partial \overline{u}}{\partial t} = G + \frac{1}{\rho_0}\frac{\partial}{\partial z}\left(\rho_0 \nu \frac{\partial \overline{u}}{\partial z}\right) - \overline{w}^* \frac{\partial \overline{u}}{\partial z} + X, \tag{A1}$$

with wave drag G, diffusivity $\nu = 0.3\,\mathrm{m^2\,s^{-1}}$, density $\rho_0 = \rho_L e^{(z-z_L)/H_\rho}$ with $\rho_L = 1\,\mathrm{kg\,m^{-1}}$, $H_\rho = 7\,\mathrm{km}$, upwelling $\overline{w}^*$, and prescribed acceleration X. The terms on the right-hand side are wave drag, vertical diffusion, vertical advection, and prescribed acceleration.

The model domain is from $z_L = 17\,\mathrm{km}$ to $z_T = 37\,\mathrm{km}$. Subscript L refers to the lower boundary, and subscript T to the upper boundary. The model is solved numerically using the Crank–Nicolson method, an implicit scheme that is second-order in space and time. The vertical resolution is $\Delta z = 250\,\mathrm{m}$.

Following Plumb (1977), the wave drag is formulated in a WKB sense where the waves are assumed to change much more rapidly than the mean wind. Each time step, the wave drag is computed as if the mean wind was constant. The model is driven by two gravity waves of equal and opposite phase speed with vertical group velocity $c_{gz} = k(\overline{u} - c_n)^2/N$ for discrete wave n, with buoyancy frequency $N = 2.16 \times 10^{-2}\,\mathrm{s^{-1}}$, wavenumber $k = 2\pi/40\,000\,\mathrm{km^{-1}}$, and phase speed $(c_1, c_2) = (-30, +30)\,\mathrm{m\,s^{-1}}$. Assuming a constant wave dissipation rate $\mu = 10^{-6}\,\mathrm{s^{-1}}$, the wave momentum flux as a function of height for a wave with source momentum flux $F_L = 0.01\,\mathrm{m^2\,s^{-2}}$ equals

$$F_n(z) = \rho_L F_L \mathrm{sgn}(c_n) \exp\left[-\int_{z_L}^{z} \frac{\mu}{c_{gz}} dz'\right]. \tag{A2}$$

The wave drag is proportional to the wave momentum flux divergence summed across all waves:

$$G = -\frac{1}{\rho_0}\sum_n \frac{\partial F_n}{\partial z}. \tag{A3}$$

The wave momentum flux is solved on half levels, as in Match and Fueglistaler (2020). The incoming wave flux into the lowest model level is prescribed. If there is a critical layer (where $u = c$) between two levels, then the momentum flux into the higher level is set to zero. The wave momentum flux divergence is computed by first-order difference.

REFERENCES

Baldwin, M. P., and Coauthors, 2001: The quasi-biennial oscillation. *Rev. Geophys.*, **39**, 179–229, https://doi.org/10.1029/1999RG000073.

Barton, C. A., and J. P. McCormack, 2017: Origin of the 2016 QBO disruption and its relationship to extreme El Niño events. *Geophys. Res. Lett.*, **44**, 11 150–11 157, https://doi.org/10.1002/2017GL075576.

Coy, L., P. A. Newman, S. Pawson, L. R. Lait, L. Coy, P. A. Newman, S. Pawson, and L. R. Lait, 2017: Dynamics of the disrupted 2015/16 quasi-biennial oscillation. *J. Climate*, **30**, 5661–5674, https://doi.org/10.1175/JCLI-D-16-0663.1.

Dunkerton, T. J., 2000: Inferences about QBO dynamics from the atmospheric ''tape recorder'' effect. *J. Atmos. Sci.*, **57**, 230–246, https://doi.org/10.1175/1520-0469(2000)057<0230:IAQDFT>2.0.CO;2.

——, and D. P. Delisi, 1997: Interaction of the quasi-biennial oscillation and stratopause semiannual oscillation. *J. Geophys. Res.*, **102**, 26 107–26 116, https://doi.org/10.1029/96JD03678.

Gelaro, R., and Coauthors, 2017: The Modern-Era Retrospective Analysis for Research and Applications, version 2 (MERRA-2). *J. Climate*, **30**, 5419–5454, https://doi.org/10.1175/JCLI-D-16-0758.1.

GMAO, 2015a: MERRA-2 inst3_3d_asm_Np: 3D, 3-hourly, instantaneous, pressure-level, assimilation, assimilated meteorological fields, version 5.12.14. GES DISC, accessed 19 August 2020, https://doi.org/10.5067/QBZ6MG944HW0.

——, 2015b: MERRA-2 tavg3_3d_udt_Np: 3D, 3-hourly, time-averaged, pressure-level, assimilation, wind tendencies, version 5.12.4. GES DISC, accessed 19 August 2020, https://doi.org/10.5067/CWV0G3PPPWFW.

Holton, J. R., and R. S. Lindzen, 1972: An updated theory for the quasi-biennial cycle of the tropical stratosphere. *J. Atmos. Sci.*, **29**, 1076–1080, https://doi.org/10.1175/1520-0469(1972)0291076:AUTFTQ>2.0.CO;2.

Li, H., R. P. Kedzierski, and K. Matthes, 2019: On the forcings of the unusual QBO structure in February 2016. *Atmos. Chem. Phys.*, **20**, 6541–6561, https://doi.org/10.5194/acp-20-6541-2020.

Lin, P., I. Held, and Y. Ming, 2019: The early development of the 2015/2016 quasi-biennial oscillation disruption. *J. Atmos. Sci.*, **29**, 821–836, https://doi.org/10.1175/JAS-D-18-0292.1.

Lindzen, R. S., and J. R. Holton, 1968: A theory of the quasi-biennial oscillation. *J. Atmos. Sci.*, **25**, 1095–1107, https://doi:10.1175/1520-0469(1977)0341847:TIOTIW>2.0.CO;2.

Match, A., and S. Fueglistaler, 2019: The buffer zone of the quasi-biennial oscillation. *J. Atmos. Sci.*, **76**, 3553–3567, https://doi.org/10.1175/JAS-D-19-0151.1.

——, and ——, 2020: Mean flow damping forms the buffer zone of the quasi-biennial oscillation: 1D theory. *J. Atmos. Sci.*, **77**, 1955–1967, https://doi.org/10.1175/JAS-D-19-0293.1.

McIntyre, M. E., 1994: The quasi-biennial oscillation (QBO): Some points about the terrestrial QBO and the possibility of related phenomena in the solar interior. *The Solar Engine and Its Influence on Terrestrial Atmosphere and Climate*, Springer, 293–320, https://doi.org/10.1007/978-3-642-79257-1_18.

Newman, P. A., L. Coy, S. Pawson, and L. R. Lait, 2016: The anomalous change in the QBO in 2015–2016. *Geophys. Res. Lett.*, **43**, 8791–8797, https://doi.org/10.1002/2016GL070373.

Osprey, S. M., N. Butchart, J. R. Knight, A. A. Scaife, K. Hamilton, J. A. Anstey, V. Schenzinger, and C. Zhang, 2016: An unexpected disruption of the atmospheric quasi-biennial oscillation. *Science*, **353**, 1424–1427, https://doi.org/10.1126/science.aah4156.

Plumb, R. A., 1977: The interaction of two internal waves with the mean flow: Implications for the theory of the quasi-biennial oscillation. *J. Atmos. Sci.*, **34**, 1847–1858, https://doi:10.1175/1520-0469(1977)0341847:TIOTIW>2.0.CO;2.

Rajendran, K., I. M. Moroz, S. M. Osprey, and P. L. Read, 2018: Descent rate models of the synchronization of the quasi-biennial oscillation by the annual cycle in tropical upwelling. *J. Atmos. Sci.*, **75**, 2281–2297, https://doi.org/10.1175/JAS-D-17-0267.1.

Renaud, A., L.-P. Nadeau, and A. Venaille, 2019: Periodicity disruption of a model quasibiennial oscillation of equatorial winds. *Phys. Rev. Lett.*, **122**, 214504, https://doi.org/10.1103/PhysRevLett.122.214504.

Tweedy, O. V., and Coauthors, 2017: Response of trace gases to the disrupted 2015–2016 quasi-biennial oscillation. *Atmos. Chem. Phys.*, **17**, 6813–6823, https://doi.org/10.5194/acp-17-6813-2017.

Wallace, J. M., R. L. Panetta, and J. Estberg, 1993: Representation of the equatorial stratospheric quasi-biennial oscillation in EOF phase space. *J. Atmos. Sci.*, **50**, 1751–1762, https://doi.org/10.1175/1520-0469(1993)0501751:ROTESQ>2.0.CO;2.

Watanabe, S., K. Hamilton, S. Osprey, Y. Kawatani, and E. Nishimoto, 2018: First successful hindcasts of the 2016 disruption of the stratospheric quasi-biennial oscillation. *Geophys. Res. Lett.*, **45**, 1602–1610, https://doi.org/10.1002/2017GL076406.